Spatial arrangement of faults and opening-mode fractures

S. E. Laubach, J. Lamarche, B. D. M. Gauthier, W. M. Dunne, David J. Sanderson

Journal of Structural Geology 108 (2018) 2–15

Contents lists available at ScienceDirect

Journal of Structural Geology

journal homepage: www.elsevier.com/locate/jsg

Spatial arrangement of faults and opening-mode fractures

S.E. Laubach [a, *], J. Lamarche [b], B.D.M. Gauthier [c], W.M. Dunne [d], David J. Sanderson [e, f]

[a] Bureau of Economic Geology, Jackson School of Geosciences, The University of Texas at Austin, Austin, TX, 78713, USA
[b] Aix-Marseille Univ, CNRS, IRD, Coll de France, CEREGE, 3 Place Victor Hugo (Case 67), 13331, Marseille Cedex 3, France
[c] TOTAL, Total EP, Tour Coupole, 2 Place Jean Millier, La Défense 6, 92078, Paris-La Défense Cedex, France
[d] Department of Earth and Planetary Sciences, University of Tennessee, Knoxville, TN, 37996, USA
[e] Ocean and Earth Science, University of Southampton, National Oceanography Centre, Southampton, SO14 3ZH, UK
[f] Faculty of Engineering and Environment, University of Southampton, Southampton, SO17 1BJ, UK

ARTICLE INFO

Article history:
Received 3 August 2017
Accepted 16 August 2017
Available online 24 August 2017

Keywords:
Cluster
Corridor
Fractal
Lineament
Mechanical stratigraphy
Spacing
Swarm
Topology

ABSTRACT

Spatial arrangement is a fundamental characteristic of fracture arrays. The pattern of fault and opening-mode fracture positions in space defines structural heterogeneity and anisotropy in a rock volume, governs how faults and fractures affect fluid flow, and impacts our understanding of the initiation, propagation and interactions during the formation of fracture patterns. This special issue highlights recent progress with respect to characterizing and understanding the spatial arrangements of fault and fracture patterns, providing examples over a wide range of scales and structural settings. Five papers describe new methods and improvements of existing techniques to quantify spatial arrangement. One study unravels the time evolution of opening-mode fracture spatial arrangement, which are data needed to compare natural patterns with progressive fracture growth in kinematic and mechanical models. Three papers investigate the role of evolving diagenesis in localizing fractures by mechanical stratigraphy and nine discuss opening-mode fracture spatial arrangement. Two papers show the relevance of complex cluster patterns to unconventional reservoirs through examples of fractures in tight gas sandstone horizontal wells, and a study of fracture arrangement in shale. Four papers demonstrate the roles of folds in fracture localization and the development spatial patterns. One paper models along-fault friction and fluid pressure and their effects on fault-related fracture arrangement. Contributions address deformation band patterns in carbonate rocks and fault size and arrangement above a detachment fault. Three papers describe fault and fracture arrangements in basement terrains, and three document fracture patterns in shale. This collection of papers points toward improvement in field methods, continuing improvements in computer-based data analysis and creation of synthetic fracture patterns, and opportunities for further understanding fault and fracture attributes in the subsurface through coupled spatial, size, and pattern analysis.

1. Introduction

During the past decade, the need for meaningful documentation and accurate prediction of fracture patterns in the subsurface has become urgent. The spatial arrangement of faults and opening-mode fractures is a key aspect of structural heterogeneity and anisotropy in the upper elastofrictional crust (Sahimi, 2011; Bear et al., 2012). Uncertainty about fundamental fault and fracture spatial patterns threatens engineering operations such as fluid injection underground (Weng et al., 2011; Dahi-Taleghani and Olson, 2011), management of induced seismicity (Rutqvist et al., 2016) and the efficiency and success of fluid extraction, for example, in unconventional and deep hydrocarbon reservoirs (Cacas et al., 2001; Solano et al., 2011; Gale et al., 2014), and geothermal systems (Vidal et al., 2017). Examples of cryptic but important arrangements include highly concentrated opening-mode fracture clusters that may locally breach reservoir cap rocks (Ogata et al., 2014), account for abrupt differences in well performance (Questiaux et al., 2010; Laubach et al., 2016), or, on broader regional scales, account for crustal fluid flow and ore deposit patterns (Jelsma et al., 2004).

Bulk rock strength and stiffness are also significantly influenced by the presence/absence of fractures and thus this attribute is sensitive to fracture patterns. At Yucca Mountain, for example, while fracture pattern characterization was important for

* Corresponding author.
E-mail address: Steve.Laubach@beg.utexas.edu (S.E. Laubach).

http://dx.doi.org/10.1016/j.jsg.2017.08.008

considering meteoric fluid and fluid containment in and near the tunnels for canister storage, it also mattered for calculating material properties during rock reheating by the canisters and for roof strength in the tunnels (Brookins, 2012).

Fault and fracture patterns also provide evidence of structural growth processes (e.g., Olson, 1993, 2004; Gillespie et al., 2017). Increasingly, quantifying spatial arrangement is central to understanding pattern origins. How do patterns relate to mechanical stratigraphy (Hooker et al., 2013; McGinnis et al., 2017), scale (Bonnet et al., 2001), loading conditions (Engelder, 1985; Gillespie et al., 2001), growth processes and rates (Atkinson, 1984; Alzayer et al., 2015), interaction with concurrent geochemical processes (Caputo and Hancock, 1998; Olson et al., 2009; Hooker et al., 2012), and other factors? Accepted concepts such as the reliability of the fracture spacing-bed thickness relationship (Ladeira and Price, 1981) are challenged by observations from the deep subsurface including horizontal wells (Lorenz and Hill, 1994; Hooker et al., 2009; Cho et al., 2013; Laubach et al., 2016) and rich new two- and three-dimensional data from outcrop imaging (Bisdom et al., 2017). These opportunities, and perceived limitations of current methods (e.g., McGinnis et al., 2015), have prompted new conceptual approaches including systematic quantification of complex patterns (Hardebol and Bertotti, 2013; Bruna et al., 2015; Sanderson and Nixon, 2015; Watkins et al., 2015; Healy et al., 2017).

Here, we introduce this special issue by summarizing how authors have addressed fault and fracture spatial arrangement. We highlight interrelations amongst their research directions. Contributions include descriptions of several new methods and new applications of recently developed methods. Papers focus on natural examples, so the active areas of stochastic, geomechanical, and mechanical-chemical modeling are not directly represented (e.g., Bai and Pollard, 2000; Bai et al., 2000; Olson et al., 2009; Ivanova et al., 2014; Hooker and Katz, 2015). Yet, improvement of the characterization of fracture patterns will provide better tests for validating future stochastic and geomechanical-chemical models. Although natural fault and fracture spatial arrangement is a broad topic, and this special issue by no means covers all the important aspects, this collection of papers points toward useful directions for further work. Among these are awareness of more complex and hierarchical patterns of fault and fracture arrangement than hitherto suspected, recommendations for data collection protocols, appreciation of input needed for models, and opportunities for synergy among different approaches to defining and understanding spatial arrangement.

2. Spacing and spatial arrangement

For faults and opening-mode fractures, *spatial arrangement* is the property possessed by an array that defines the position of constituent structures in the rock mass (Fig. 1). Interpreted broadly, spatial arrangement is nearly synonymous with the field of structural geology—the arrangement of the parts of a rock mass, irrespective of scale, including spatial relationships between parts, their relative size and shape and the internal features of the parts (Brodie et al., 2007).

This has led to two somewhat different ways of viewing the spatial arrangement of fractures:

1) As objects in space, where the position, orientation and abundance of the fractures are measured, usually in some geographical reference frame. This is what practitioners generally apply, and includes whether faults and fractures are closely or widely separated—their pattern of abundance—and whether they are regularly spaced or not (Fig. 1).
2) As objects in relation to one another, i.e. the topology (Sanderson and Nixon, 2015). Such measures are independent of scale and orientation, and remain invariant under any continuous affine transformation (Fig. 2).

In both cases, related issues are how patterns correlate and/or interact with host rock attributes, associated folds and faults over a range of scales, and with formative processes. This special issue covers aspects of all of these topics.

2.1. 1-D (scanline) sampling

Owing to the limited view of fracture patterns afforded by most subsurface probes (Narr, 1996) or outcrops (Zeeb et al., 2013), a

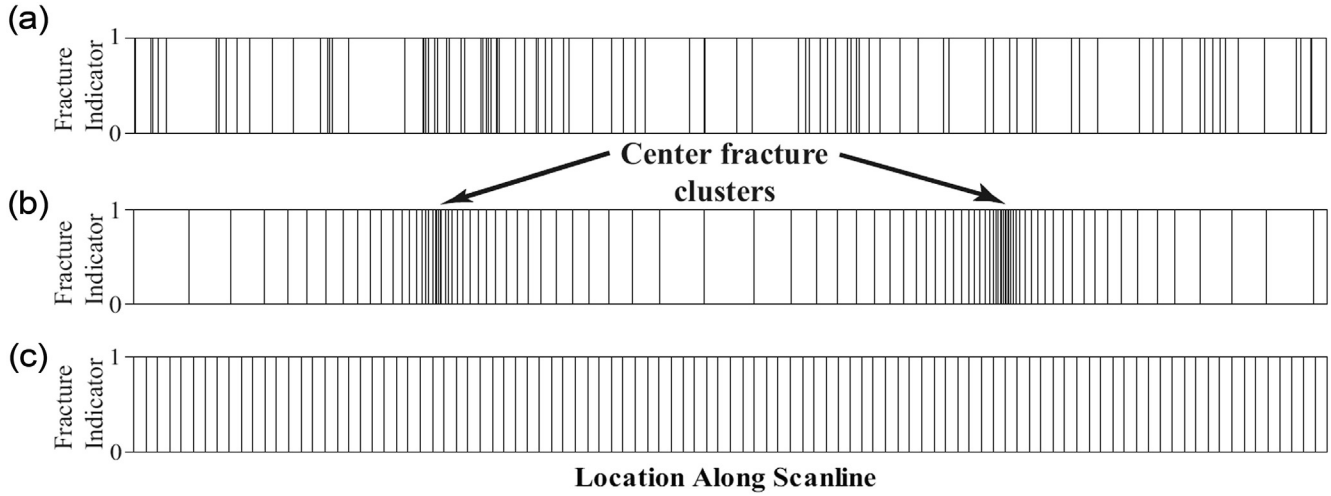

Fig. 1. Fracture indicator series of three synthetic data sets with identical numbers of fractures (100) and scanline lengths. Indicator series equals 1 (black) where a fracture is present along scanline and 0 (white) where there is no fracture. All fracture apertures are equal and infinitesimally small and therefore can be ignored. (a) Randomly located fractures show several places where fractures are more closely spaced (clusters) but clusters are not statistically significant. (b) A synthetic data set with the same values of fracture spacing as in a) but sequenced in such a way that two statistically significant fracture clusters are present. Spacings between fractures systematically increase away from center of each cluster. (c) Regularly spaced fractures for which spacing between all pairs of nearest-neighbor fractures is constant. Statistics that describe useful aspects of spacing include the mean, which governs overall expected frequency of intersection, as well as the standard deviation, which describes spatial regularity. That is, a hypothetical fracture set may be perfectly regularly spaced, or highly clustered, with statistically random spacing occupying an intermediate position on the spatial regularity spectrum. Figure courtesy of R. Marrett.

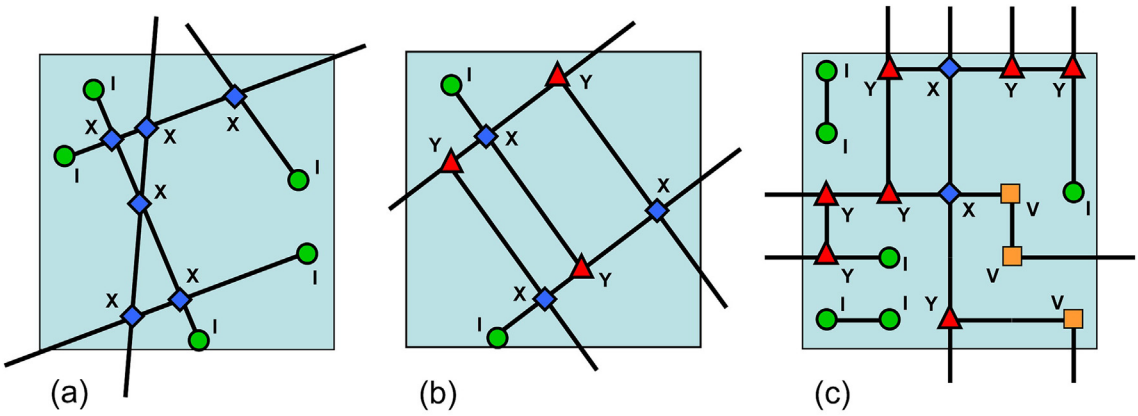

Fig. 2. Network topology defined by the arrangement of lines and nodes: (a) random array of lines as generated in stochastic models; (b) schematic representation of a fracture network; (c) network generated by random selection of branches on a square grid. From Sanderson and Nixon (2015).

common and convenient data source is one-dimensional (1-D) measurements along a straight line of observation, or *scanline*, orthogonal to fracture strike. Widely used measurements are *spacing* (Priest and Hudson, 1976; La Pointe and Hudson, 1985), the perpendicular distance between two features of the same orientation sets or nearest neighbor distance, and *intensity*, the number of fractures per unit length. For a line, intensity is simply the inverse of average spacing. A byproduct of this approach is straightforward and quantitative comparison of subsurface patterns, which are almost invariably 1-D data, with outcrop data and models that generate artificial networks.

Measures of spacing include average, median, standard deviation, ratio of standard deviation to mean (coefficient of variation, Cv) (e.g. Gillespie et al., 1999; 2001), and discrete and cumulative frequency distributions (e.g. Narr and Suppe, 1991). Among these techniques, coefficient of variation and interval counting (e.g. Gillespie et al., 1993; Walsh and Watterson, 1993) are least affected by the minimum size, or threshold, of fractures sampled. The other techniques are strongly scale-dependent, because spacing values change significantly with threshold (Ortega et al., 2006; Roy et al., 2016). Consequently, most analyses of spacing, or of spatial arrangement, are only meaningful if the size range is stated for measured fractures. For subsurface situations, where narrow fractures may be preferentially sealed with natural cements (i.e., Laubach, 2003; Olson et al., 2009), the most meaningful measure for fluid flow or fracture strength is the spatial arrangement of fractures at or above a threshold size.

In studies of opening-mode fractures, spacing has long been a standard measurement, probably because joints, the ubiquitous barren opening-mode fractures near Earth's surface, commonly show regular spacing (Figs. 3 and 4) (Ladeira and Price, 1981; Narr and Suppe, 1991). Moreover, joints normally show a proportionality between *average* fracture spacing and fractured-layer thickness (e.g. Ladeira and Price, 1981; Huang and Angelier, 1989; Narr and Suppe, 1991; Gross, 1993). Experiments and mechanical models account for the proportionality (e.g. Bai et al., 2000). Built into widely used subsurface fracture assessment methods is a presumption of regular (or random) spacing (Narr and Lerche, 1984; Wehunt et al., 2017). As papers in this special issue demonstrate, regular spacing is not a safe assumption for subsurface fractures.

Faults generally have *irregular spacing* and fracture clusters—defined as areas of anomalously close fracture spacing (Peacock et al., 2016). Such patterns are also present in opening-mode fractures, termed joint and vein arrays (e.g., Delaney et al., 1986; Odling, 1992; Belgrano et al., 2016), corridors (Singh et al., 2008; Questiaux et al., 2010) or swarms (Laubach et al., 1995; Gabrielsen and Braathen, 2014) (Figs. 5 and 6). Mechanical models can also account for local, anomalously close spacing (e.g., Olson, 2004).

Irregular spacing can be quantified using coefficient of variation, or ratio of standard deviation to mean, from nearest-neighbor fracture spacings (Gillespie et al., 1993). Cumulative frequency plots also allow statistical testing, for example against uniform distribution on the line, using non-parametric tests based on Kuiper (1960) and Stephens (1965), as discussed by Putz-Perrier and Sanderson (2008a). These approaches have been applied to veins (Sanderson et al., 1994), faults, and structures within fault damage zones (see Putz-Perrier and Sanderson, 2008a,b; 2010; Schöpfer et al., 2016; Choi et al., 2016). Anomalously closely spaced fractures are not necessarily the same as clusters of *interconnected* fractures (Manzocchi, 2002).

Scanline sampling is subject to well-known censoring and truncation artifacts caused by the limits of sampling dimension and geometry (Terzaghi, 1965; Pickering et al., 1995; Ortega et al., 2006). Censoring artifacts are widespread because limited scanline length leads to undersampling of rare large structures. Statistical tests and uncertainty assessments can optimize scanline data analysis (Guerriero et al., 2011; Santos et al., 2015; Rizzo et al., 2017).

As noted in this volume (Marrett et al., 2017) and elsewhere (Putz-Perrier and Sanderson, 2008a; Roy et al., 2010, 2014) spatial arrangement might show organization, in which case some aspects of arrangement may be predictable, or it might lack organization, implying an arrangement that is statistically indistinguishable from random positioning. Arrangements differ from random by being more clustered or more regularly spaced. Although random arrangements show clusters (Priest and Hudson, 1976), non-random arrangements can be either even more strongly clustered, positively or negatively compared with random (Fig. 1). The latter situation arises for spacing that is *more regular* than expected for a random arrangement. *Spatial organization* implies objects are spatially organized and thus arranged non-randomly. Spatial organization is a special case of spatial arrangement, possibly arising as an emergent property of a self-organized system or imposed by some other aspect of the geology, such as host rock type and dimensions, diagenetic overprint, or position in folds. This volume treats aspects of all of these potential influences on spatial arrangement.

2.2. 2-D and 3-D sampling

The advent of widely available high-resolution imagery including LIDAR surveys and UAV photogrammetry (e.g., Bemis et al.,

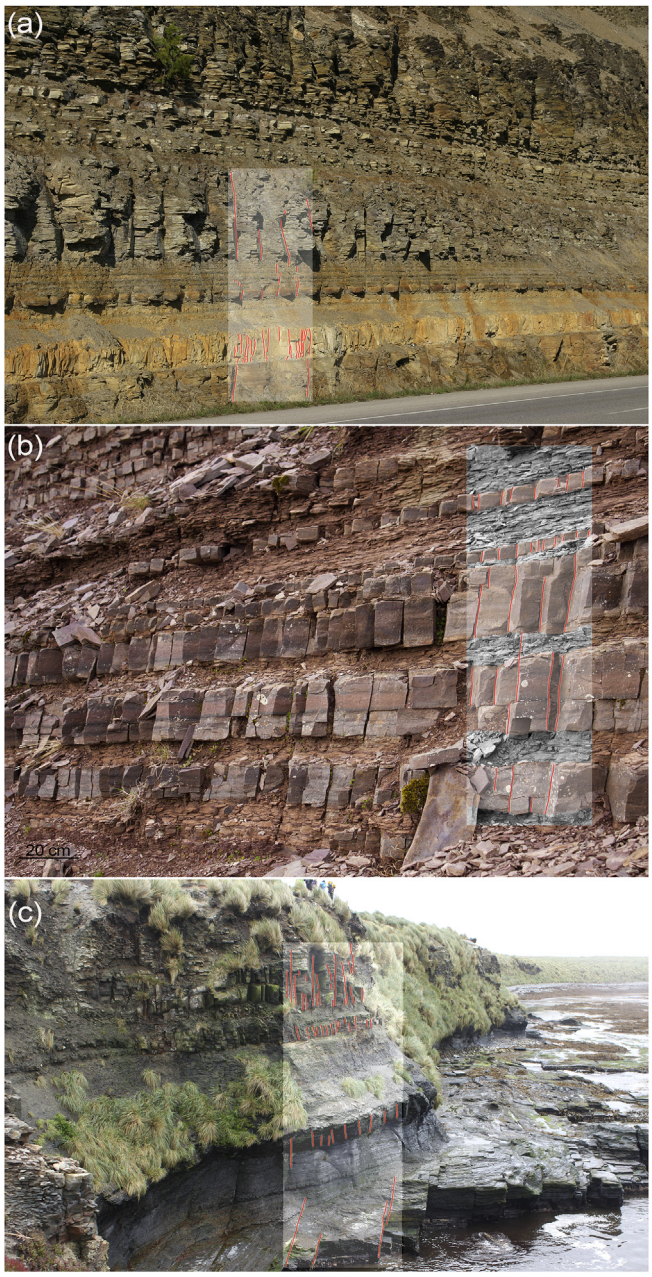

Fig. 3. Regularly spaced opening-mode fractures with bed-bounded height patterns. Insets highlight trace patterns in cross section. (a) Devonian New Albany Shale, eastern Kentucky, view northeast. (b) Precambrian Applecross Formation sandstone and shale, Scotland. View northeast. (c) Carboniferous/Permian Lafonia Group sandstone and shale, Sea Lion Island, Falkland Islands. View north. For fractures in many outcrops, opening-mode fracture growth in stratified rocks is height-restricted and fracture spacing scales with the height of fractures, resulting in regular spacing (Schöpfer et al., 2016).

2014; Vollgger and Cruden, 2016) allows capture of rich fracture pattern information from outcrops (Lamarche et al., 2017a). The concepts of intensity and spacing can be extended to higher sampling dimensions. In 2-D, measurement is usually of maps or surface outcrops, with intensity being measured as trace length per unit area. If outcrop quality permits, such basic imagery allows spatial arrangement studies to go beyond 1-D scanlines, making systematic quantification of complex patterns practical (Hardebol and Bertotti, 2013; Sanderson and Nixon, 2015; Watkins et al., 2015; Healy et al., 2017). A recent development is systematic characterization of the geometric arrangements of faults and fractures with respect to one another (Anderson et al., 2013; Kruhl, 2013; Sanderson and Nixon, 2015). These topological methods are useful ways for describing the characteristics of networks. This volume contains one example of this approach (Procter and Sanderson, 2017). A byproduct of this approach is more straightforward and quantitative comparison of real patterns and models that generate artificial networks.

The extension of sampling to 3-D is mainly confined to seismic imaging of faults, although CT-scanning of core and rock samples and sequential thin sections are extending the range of 3-D data to microscopic scales (Anders et al., 2014). In 3-D circumstances, intensity can be defined as surface area per unit volume, and spacing or block size as its inverse. Note that in 1-D, 2-D and 3-D, intensity always has dimensions of [length]$^{-1}$ and spacing of [length]. Other forms of imaging, such as well-bore imaging and Lidar scanning, collect data from more complex, non-planar surfaces that are essentially between 2-D and 3-D representations of fractures.

In two dimensions the combined effects of geometry and topology are clear. In Fig. 7 we show a typical natural fracture network (Fig. 7a) consisting of two sets of fractures at approximately 90°, which we will assume to be conductive. The same fracture traces (i.e. same lengths and orientations) are rearranged to form a 'fracture corridor' (Fig. 7b), a random arrangement (Fig. 7c) and with one set cemented (dashed lines in Fig. 7d). In Fig. 7a, c, d the spatial distributions are homogeneous, whereas in Fig. 7b there is a spatial clustering in the fracture corridor. In these four networks the geometry is identical, but the topology different, as seen by the different proportions of node types (Fig. 7e). If we just consider the conductive components, then the fractures in networks a) and b) connect across the area and flow would be enhanced, whereas the fractures do not form a spanning network in Fig. 7c, due to their I-dominated topology), and in Fig. 7d, where one set is non-conductive (cemented) and isolates the conductive fractures. Another set of configurations is shown by Olson et al. (2010; their Fig. 7) where fracture shape—narrow fracture tips—affects where cement closes fractures, rendering a physically continuous network discontinuous for flow. These simple schematic diagrams illustrate the key roles played by geometry, topology, spatial arrangement and conductivity of the fracture elements in determining the behavior of the network. A natural subsurface example of orthogonal sets of clustered, and partly cemented fractures is described by Laubach et al. (2016).

2.3. Layering and fracture height

An aspect of fracture spatial arrangement that is rarely explicitly accounted for in outcrop studies of bedded rocks is fracture height, or fracture height patterns. Stratified rocks in outcrop commonly have fracture heights that are restricted to specific beds (Fig. 3) and may also have regular spacing (e.g., Ladeira and Price, 1981; Narr and Suppe, 1991). Considerable work has gone into explaining how fracture spacing scales with fracture height, resulting in regular spacing (Schöpfer et al., 2016). Only recently has a height classification been proposed (Hooker et al., 2013) and few field studies rigorous describe or classify height patterns. Yet differences in height patterns, particularly if undiagnosed, can render outcrop fracture spacing data meaningless and interfere with comparison of field data with models, which commonly assume perfect bed-bounded patterns, a mere end member of natural height patterns. Some studies specify which fractures have been included and which omitted (Fig. 4), but if hierarchies of fracture heights are present, spatial arrangements along any given horizon may contain fractures that reflect different scales or hierarchies of mechanical stratigraphy.

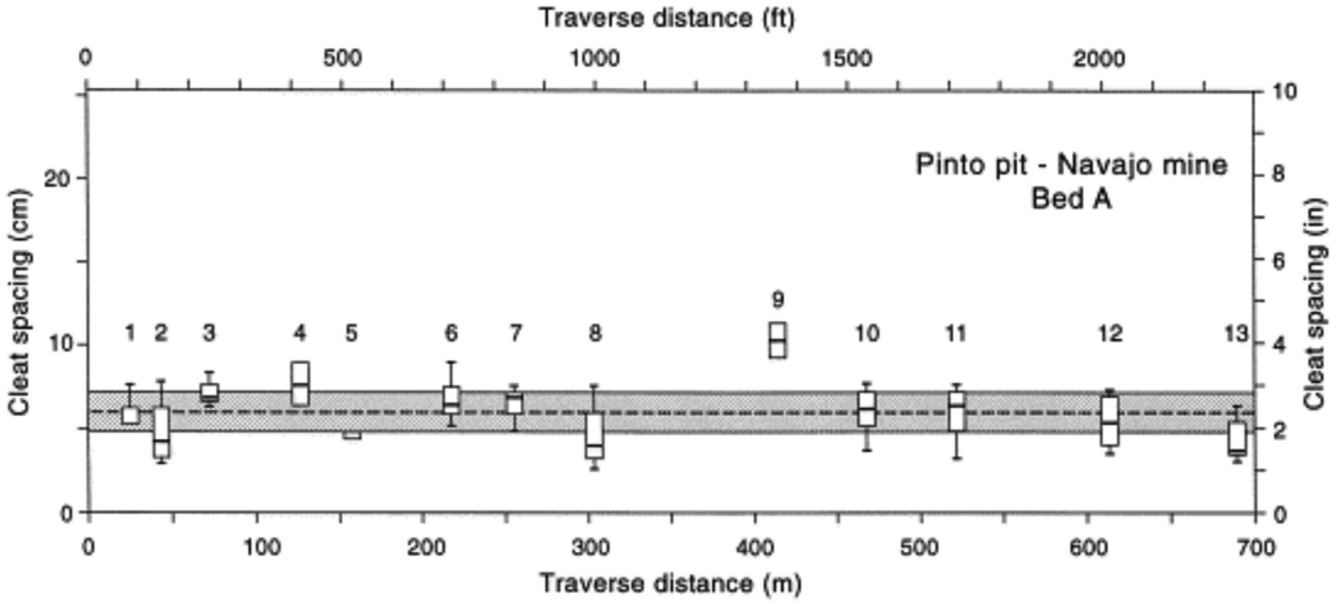

Fig. 4. Opening-mode fracture (cleat) spacing versus traverse distance in a bed of uniform dip, thickness, and composition, San Juan Basin, New Mexico. Fractures in coal typically have a wide range of sizes. In this example, the wide size range was accounted in spacing analysis by measuring only those fractures that extend from top to base of the fractured layer, ignoring shorter fractures. Nevertheless, spacing values in equal-sized bins show statistically significant fluctuations in average spacing values. Center half of data at each station is shown by box, and median by bar. Dashed line and shaded area are mean and one standard deviation of measurements from all stations. Measuring spacing in this way matches assumptions of some numerical models for fracture spacing patterns. From Laubach et al. (1998). Compare with results from Procter and Sanderson (2017), this volume.

In both stratabound and non-stratabound fracture sets, many highly clustered and non-random fracture patterns have been identified (see literature review in Hooker and Katz, 2015). Methodological and modeling studies note the importance of the 3-D aspect of fracture patterns (Priest, 1993; Dershowitz et al., 2000; Mauldon et al., 2001), but this attribute has had insufficient attention in outcrop and subsurface studies. To the extent allowed by inherently limited samples, we need records of height patterns for subsurface fracture arrays (for example, the top-bounded fracture in Fig. 6) as well as systematic records of these patterns in outcrop. Papers in this volume account for fracture height patterns in unraveling spatial arrangement and fracture origins (Lavenu and Lamarche, 2017; Korneva et al., 2017).

2.4. Faults and damage zones

Both surface and sub-surface mapping have shown that there is a wide range of spatial arrangement for faults and fractures associated with folds (e.g., Couples and Lewis, 1998). Clustering is prominent in some fault patterns (Bour and Davy, 1999). Even in regional joint systems there are commonly well-developed, but poorly understood, fracture corridors. One of the most widely recognized spatial arrangements occurs in fault damage zones, where regions of intense fracturing occur around the cores and slip surfaces of faults. The damage can take the form of additional synthetic and antithetic faults, deformation bands, veins or pull-aparts, and/or opening-mode fractures (Chester and Logan, 1986; Kim et al., 2004). Damage is generally interpreted as due to the initiation, propagation, interaction and build-up of slip along faults (Cowie and Scholz, 1992; Kim et al., 2004; Choi et al., 2016).

The pattern, size, and spatial arrangement may also be modified by host rock composition, either through the effect of composition on mechanical properties, or via the influence on host-rock composition on diagenesis (Laubach et al., 2014). Where damage zones are concentrations of faults, deformation bands and fully cemented veins they may provide important sealing capacity, but where open or partially cemented fractures occur they provide fluid pathways along faults. Both sealing and conductive fractures can develop together in the same fault zone (e.g. Aydin, 2000; Jourde et al., 2002; Matonti et al., 2012; Laubach et al., 2014).

From a practical standpoint, predicting how these linked kinematic, mechanical, and geochemical processes affect fault properties is important. Even for faults visible using remote sensing and geophysical probes, imaging is usually inadequate for revealing fine-scale attributes that affect fluid flow and fault strength. These linked issues are only beginning to be explored with the intensity that they deserve.

3. Spatial arrangement and chemical processes

Most opening-mode fractures and faults in *subsurface* bedded rocks, or fractures that formed in the subsurface, contain some amount of cement (i.e., Evans, 1995; Laubach, 2003; Holland and Urai, 2010; Evans and Fischer, 2012; Gale et al., 2014). Within a given set of fractures, fractures may be open and 'joint like', with deposits that are thin and inconspicuous. However, elsewhere, fractures of that set may be sealed. The pattern of sealing may depend on fracture age or location, the thermal or fluid-flow history of the fractures, or merely the fracture size or rate at which fractures opened (Laubach, 2003; Hilgers et al., 2006; Lander and Laubach, 2015, Vandeginste et al., 2015; Ankit et al., 2015; English and Laubach, 2017). For such fractures, the terms 'joint' and 'vein' are inconvenient descriptors. Instead, it is preferable to specify the displacement mode, which can be observed, and explicitly describe the mineral fill. An increasing appreciation that joints formed under cold conditions near the Earth's surface, and fractures formed at depth have many important differences (Peacock, 2004) needs to be taken into account in spatial arrangement studies.

Some evidence from field investigations (Hooker et al., 2013) and numerical models (Hooker and Katz, 2015) suggest that fracture spatial arrangement, as well as other attributes, may vary with the amount of cement in fractures at the time of fracture growth. In

Fig. 5. Clustered opening-mode fractures and small faults, Miocene Monterey Formation. Inset shows fracture occurrence versus distance plot. Notice light-colored alteration near clustered fractures due to groundwater flow. A, altered; uA, unaltered rock. Many highly clustered, and demonstrably non-random, fracture patterns have been identified, both in stratabound and non-stratabound fracture sets and in both outcrop and subsurface data. In this volume, Li et al. (2017) show that locally in the subsurface, two sets of orthogonal fractures in the Frontier Formation are highly clustered.

other words, the mechanical effects of the cement deposits interfere with and modify how fracture patterns develop. In this volume, Li et al. (2017) found markedly differing fracture spatial arrangement in the same formation. Differences correlate with the types and amount of fracture-filling cement at the time of fracture growth. The chemical processes of diagenesis also change rock mechanical properties. Consequently, when a fracture pattern forms relative to these geochemical changes likely affects the fracture patterns that form. In this volume, Lavenu and Lamarche (2017) describe fracture patterns that formed under early diagenetic conditions, and in a separate study of similar composition rocks, Korneva et al. (2017) describe the contrasting patterns of late-formed fractures. Chemical effects can also lead patterns of fracture permeability and porosity that do not match fracture abundance and size patterns. In this volume, investigating fractures in a fold-thrust belt, Watkins et al. (2017) describe large clustered fractures that are sealed. Sparse, disseminated fractures in less-deformed parts of the structure are open and more likely to have been fluid-flow conduits.

Cement textures and fluid inclusions also can provide evidence of timing within arrays of parallel fractures. In this volume, Hooker et al. (2017) use fluid inclusions in fracture cement to reconstruct how clustering arises.

4. Numerical models

Numerical models are vital tools for understanding fracture spatial arrangement. For example, the origin of clustering has been the topic of model studies (Figs. 8 and 9) (Rives et al., 1992; Renshaw and Pollard, 1994; Olson, 2004; Olson et al., 2009; Hooker and Katz, 2015; Myers et al., 2017; Yılmaz et al., 2017). Spatial arrangements of opening-mode fractures can be strongly modified by stress perturbations near faults (Rawnsley et al., 1992). Maerten et al. (2017) describe along-fault friction and fluid pressure effects on the spatial distribution of fault-related fractures. The study demonstrates the importance of local fluid pressure patterns along faults on the patterns of opening-mode fractures. Using the Boundary Element Method, the study shows how complex and realistic fault models can be constructed, and the effects of displacements, tractions, cohesion, friction, and fluid pressure investigated.

5. Papers in this volume

5.1. New and newly tested methods

In spite of being an intuitively useful concept, clustering has been resistant to effective quantification. However, without quantification, achieving rigorous comparisons of spatial arrangements is challenging. Methods are needed to distinguish fracture patterns in different rock units and structural settings where spatial periodicity or clustering is present and varies from fracture set to fracture set within the pattern, and to distinguish signal from random fluctuations. Marrett et al. (2017) present new techniques that quantifies spatial arrangement across broad ranges of length scale for structures observed in scanlines (and in principle in other sampling modes), and demonstrates the simple physical meaning of results from the techniques. The normalized correlation count technique provides a quantitative analysis of the degree to which fractures are clustered, and can distinguish between even spacing, clusters arising due to random spacing, and clustering that is stronger than a random signal.

Normalized correlation count uses spacing measurements between all pairs of fractures including non-nearest neighbors—the sequences of spacings—as well as other attributes such as size. Accounting for sequences and sizes provides information on cluster distribution and cluster internal structure. A freely available computer program, CorrCount, provided along with the paper, gives analytical and Monte Carlo solutions for randomized input spacings, allowing construction of 95% confidence intervals for the randomized sequence. If a length scale's corresponding correlation count falls either above or below the upper or lower confidence limits, the corresponding fracture spacing is statistically significant. Marrett et al. provides a way to be quantitative about fracture clustering.

Geostatistics is a foundational tool for geosciences. Yet, too many structural geologists are unaware or only mildly aware of its significance and power. Hanke et al. (2017) describes a new directional semivariogram analysis method to identify and rank the controls on the spatial variability of map-scale fracture network attributes in the Paradox Basin, Utah. This paper provides a tutorial on use of semivariograms and shows how to quantify fracture density and intersection density on a GIS-based data set comprising roughly 1200 fractures bounded by a map-scale anticline and

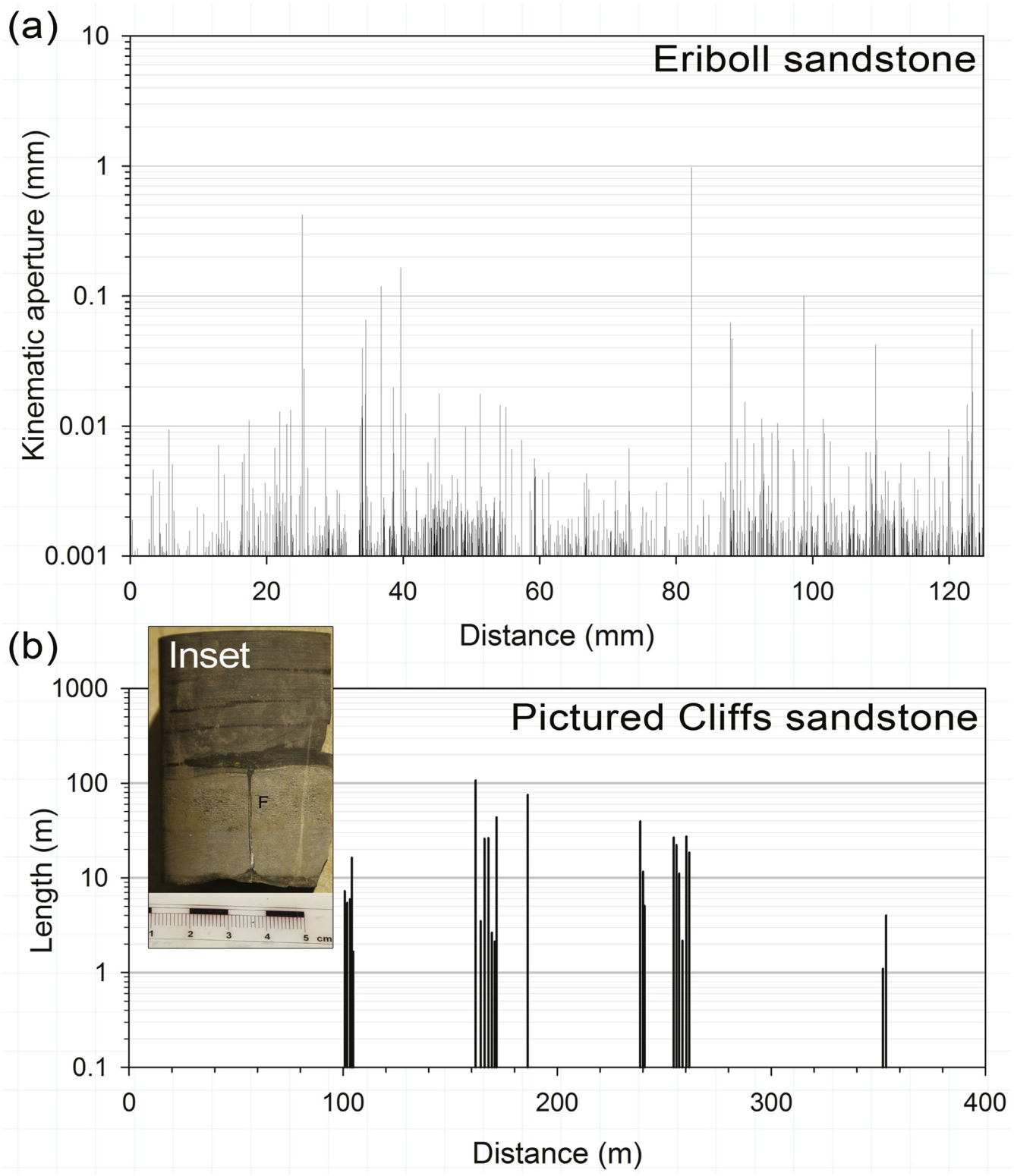

Fig. 6. Fracture spatial arrangement and size. (a) Microfracture kinematic aperture size-distance plot, quartz-filled microfractures, showing apparent clusters. Data from Gomez and Laubach (2006). (b) Length-distance plot, opening-mode fractures, Cretaceous Pictured Cliffs Formation, Colorado. Maximum fracture trace lengths are limited by outcrop size. Data from Laubach (1992). Determining if uneven fractures size and spacing patterns like these are statistically more or less clustered than random is a goal of analysis described by Marrett et al. (2017). Inset shows fracture in New Albany shale, illustrating the challenge of documenting spatial arrangement from vertical core observations.

kilometer-scale normal fault. The analysis shows that the amount and structure of spatial variability change systematically with distance from a fault, whereas the fold sets the background structure of variability. Once documented, spatial variability structure implies the geological or geomechanical causes of the heterogeneity, and provides quantitative information that can be included in predictive stochastic models.

Procter and Sanderson (2017) applied topological approaches to

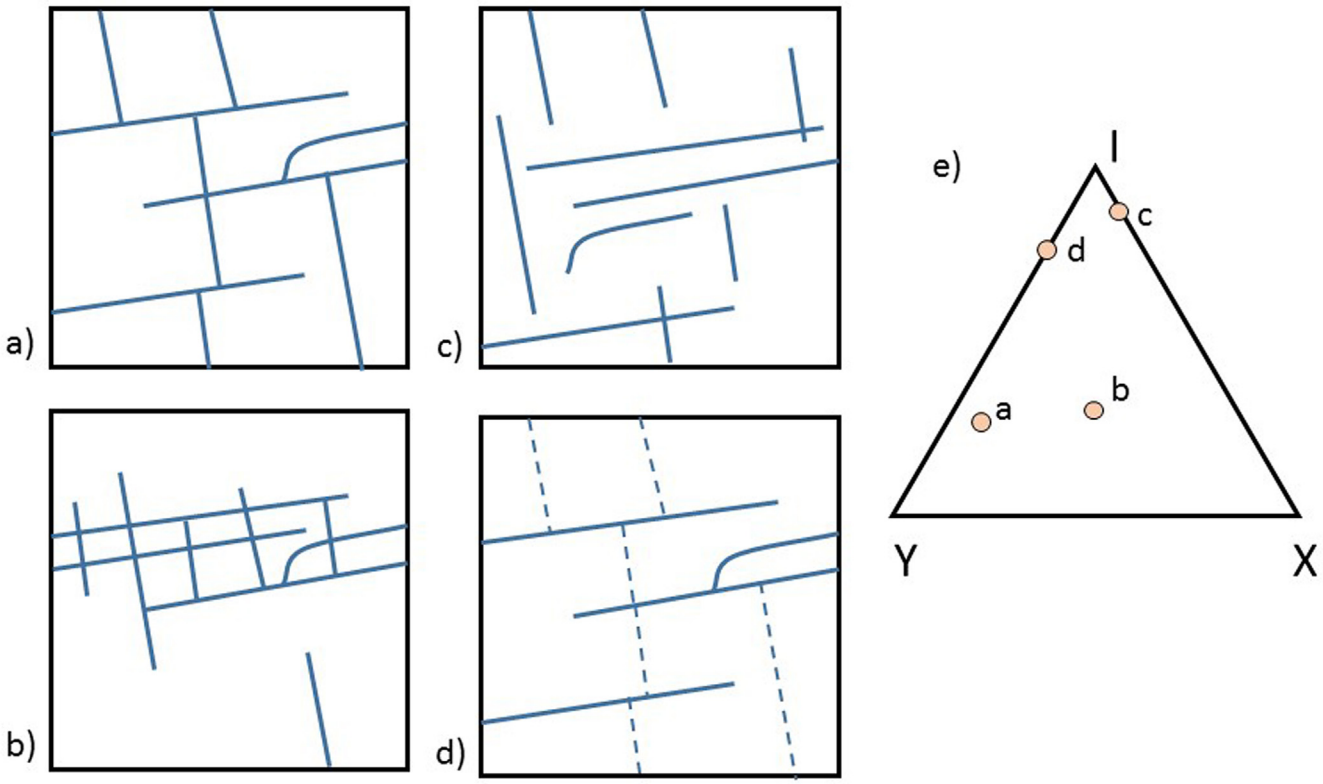

Fig. 7. Different spatial arrangements of fractures with same geometrical properties, i.e. fractures with same trace lengths and orientations arranged in 2 sets at ~90°. (a) 'natural' well-connected network; (b) same fractures clustered into a 'fracture corridor'; (c) same fractures randomly arranged; (d) as (a) with one set of fractures cemented (dashed). (e) Proportions of I-, Y- and X-nodes for conductive elements in different fracture networks; note (a) and (b) have high proportion of connected nodes (Y + X) whereas (d) and (c) have dominance of I-nodes (unconnected).

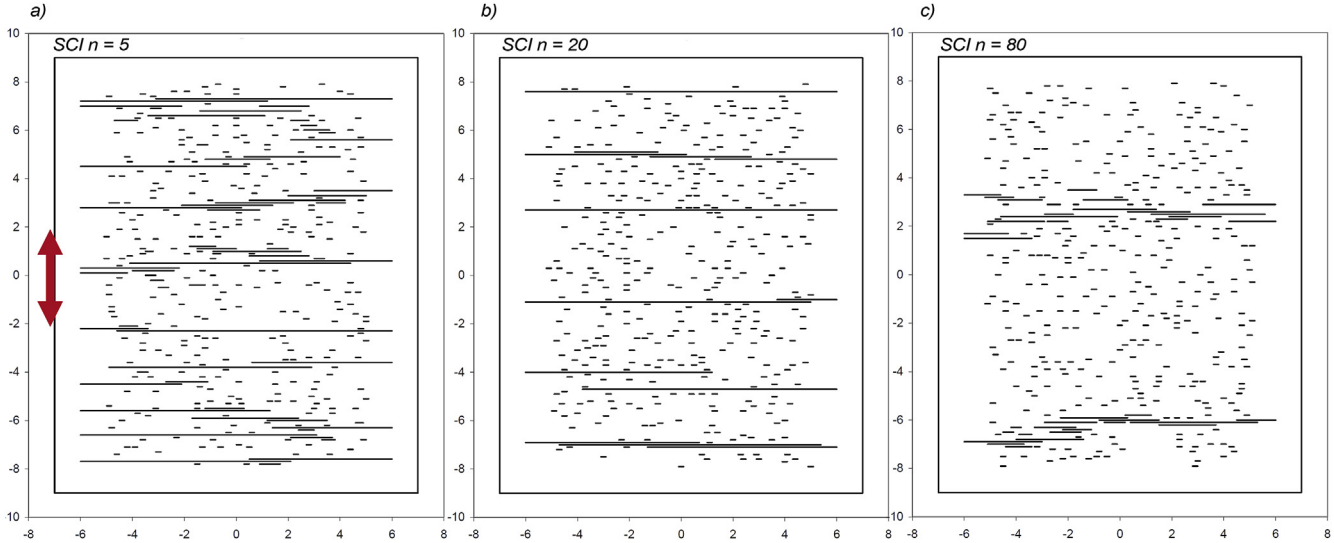

Fig. 8. Regularly spaced and clustered fractures generated in geomechanical model. Examples of subcritical fracture growth for subcritical crack indices n of (a) n = 5, (b) n = 20 and (c) n = 80. All simulations started with the same randomly located parallel flaws (short lines), a layer thickness of 8 m (dimension marked by double-headed arrow), Young's modulus of 20 GPa and Poisson's ratio of 0.25. Strain was imposed by normal displacement in the y-direction at a strain rate of 2.0×10^{-20} s^{-1} to an ultimate extension of 9×10^{-5}. Boundary conditions on the right and left of the body have zero normal displacement and all boundaries have zero shear stress. Long lines show fracture traces in plan view, and grid shows scale in meters. Modified from Olson (2004). Models that incorporate cement infilling during fracture growth produce different patterns, Olson et al., 2009.

understand spatial and layer-controlled variability in a fracture network. Topological sampling based on node counting and circular sampling areas measures fracture intensity in a layered limestone/shale sequence in well-exposed outcrops in north Somerset, UK. The approach provides similar levels of precision as scanline sampling, but is faster and allows characterization of connectivity. Also used were georeferenced photographs that allowed later measurements of trace lengths and orientations. Statistical tests

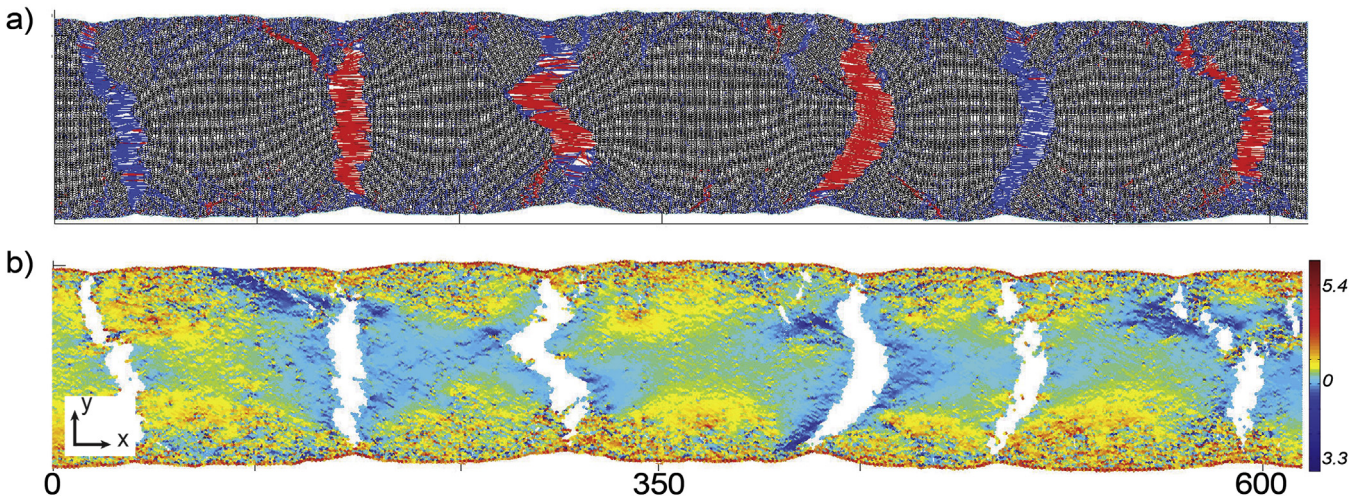

Fig. 9. Spring-lattice model showing the effect of concurrent cementation on fracture spacing. Modeled 2-D layer is stretched at a fixed rate; springs have variable elastic constants and critical breaking lengths. Simulating cement deposition concurrent with fracture opening, springs break and become re-attached by growing cement along them during layer extension. (a) After coeval stretching-induced fracturing and cementation, springs are unbroken (black), broken (red) or re-attached (blue). (b) Stress map; higher tension in the x-direction is shown in warmer colors. Note the areas of low tension around fractures are diminished where fractures are cemented. This diminishing is a consequence of re-attachment of springs and the corresponding tension developed across cemented fractures. From Hooker and Katz (2015).

confirm within-layer, between-layer, and between-locality variation in fracture intensity. Different layers have anomalous intensity at different locations, patterns not obviously related to bed thickness or compositional or textural variation between the limestone beds. Results underline the value of topological analysis in outcrop fracture surveys.

Focusing on cluster development in opening-mode fractures that are fully or partially filled by quartz cement and that demonstrably formed in the subsurface, Hooker et al. (2017) shows how an array of fractures starts from an unorganized flaw distribution and produces a non-random pattern. With the goal of testing the relative importance of flaw distributions, sedimentary features, structures, and self-organization to the development of natural fracture patterns, this study presents microfracture spacing measurements, compiled from eight formations on three continents using the same data collection method and scale of observation. Spacing statistics test whether microfractures are more or less clustered than would be predicted by a random arrangement of fractures.

For one data set, the Hooker et al. study goes beyond statistics to fracture spacing *evolution*, using fluid-inclusion microthermometry and thermal history modeling to reconstruct for the first time the opening history of a cluster of fractures. A comparison of results to previous models of fracture propagation supports models in which fracture clustering is the result of dynamic crack interaction during propagation. The demonstration of independent timing evidence for a group of parallel, co-genetic fractures shows how other fracture spatial arrangement histories could be reconstructed. Such records can help model development.

The paper by Snyder and Waldron (2017) uses a Markov chain analysis modified to statistically test the randomness of fracture relative timing relationships and determine a history of fracture development. This process provides a statistically tested way to interpret fracture sequence in outcrop and core. Data were collected from coastal outcrops and from cores from across the Windsor-Kennetcook subbasin in the Maritimes Basin (Canada), using the circular scanline and vertical scanline methods in outcrop, and microresistivity images and core. The results of the Markov chain analysis suggest that fracture initiation is related to dextral motion on the Minas Fault Zone, a late Paleozoic transform fault, followed by sinistral reactivation during Atlantic opening. Among eight dominant fracture sets, four reflect late Paleozoic dextral motion on the Minas Fault Zone and four reflect Mesozoic reactivation during Atlantic opening.

5.2. Opening-mode fractures

Although commonly ascribed to tectonic events, fractures occur in otherwise undeformed rocks. Lavenu and Lamarche (2017) explore patterns of such early-developed background fracture networks at regional scale using outcrops in the Provence, SE France, and the Apulian platform, SE Italy. The study highlights the critical role of evolving mechanical stratigraphy in governing the spatial arrangement of fractures in a stratigraphic reference frame. High-angle-to-bedding opening-mode fractures and bed-parallel stylolites developed synchronously during the early burial and prior to major tectonic events. During early diagenesis facies transitions did not act as mechanical discontinuities to height growth, so in a bed-normal direction fractures are unbounded. This spatial distribution differs from what would be expected from the *current* mechanical stratigraphy, where differential compaction and cementation led to marked mechanical property stratification. Diagenesis and sedimentary facies are responsible for evolving brittleness and mechanical layering in carbonates and other rocks. Lavenu and Lamarche's study shows how fracture occurrence partitions within a stratigraphic sequence, in other words, the fracture stratigraphy, is sensitive to this history. Prediction of critical fracture attributes such as the spatial pattern of height distribution needs to take this sensitivity to diagenesis into account.

Korneva et al. (2017) explore the effects of dolomitization on petrophysical properties and fracture distribution within rift-related carbonates, Hammam Faraun Fault Block, Suez Rift, Egypt. The challenge is the relationship between dolomitization, petrophysical properties fracturing, and, how these relate to the initial textural properties of the precursor limestones. Stratabound and massive dolomitization affected the petrophysical properties and fracture spacing in limestones in different ways. Here, current day mechanical stratigraphy strongly affects fracture spacing owing to the marked effect of dolomitization and its interplay with porosity variation on mechanical properties. Knowledge of the grain size and texture of precursor limestone and the crystal size of resultant dolostones are critical to predicting the rock mechanical properties

of this partially dolomitized succession. Together with the Lavenu and Lamarche (2017), this study illustrates the importance of understanding the mechanical property history in interpreting fracture abundance patterns.

Because of limited access to large vertical exposures, fracture studies from analogues are commonly limited to small outcrops that restricts measurement of joint sizes to relatively small length scales. Hence, the distribution of large through-going joints and their relation to thick mechanical units, remains poorly studied. Corradetti et al. (2017) describes the distribution and arrest of vertical through-going joints in a reservoir-scale carbonate platform exposure, Sorrento peninsula, Italy, made of shallow water carbonate and dolomite layers in alternation. To record all fracture scales within this large outcrop, the authors used drone-aided photogrammetric techniques to produce a Virtual Outcrop Model (VOM) of an inaccessible cliff 250 meters wide and >200 meters high, complemented by local field stratigraphic and stratimetric measurements. One thousand and three georeferenced through-going fractures were documented by manual digitization of points along fracture and bedding traces. Major bed-perpendicular through-going fractures are more likely to arrest in the shallow-water carbonate sequence. The analysis of the VOM show that the sedimentary units have a hierarchy of mechanical behaviors and that the scale and vertical continuity of through-going joints and fracture stratigraphy reflects these mechanical properties in a complex height hierarchy.

Focusing on subsurface data, Li et al. (2017) quantifies opening-mode fracture spatial organization of a tight-gas sandstone for both surface and subsurface using horizontal wellbore image logs, core and outcrop. The example is Upper Cretaceous Frontier Formation tight gas sandstones in Wyoming. Using Marrett et al.'s (2017) normalized correlation count method and software, Li et al. found that clustered subsurface fracture patterns differ from regularly spaced surface patterns. The reservoir contains clusters of open fractures in two orientations. For the best-characterized set, clusters are likely fractal with 35 m-wide clusters separated by 50–100 m gaps. Cluster patterns can account for gas and water production anomalies. Rapid clustering analysis using horizontal image log observations is feasible with the correlation count software. Causes of differing clustering patterns likely reflect differences in degree of diagenesis and structural setting between outcrop and subsurface localities.

Ladevèze et al. (2017) define the natural fracture network in eastern Canada in sedimentary rocks comprising shallow aquifers, as well as in Utica Shale, a gas play, with the aim of understanding fracture networks potentially linking aquifers with rocks at depth. The study used outcrop data and image-log analysis from eleven shallow wells. Here, outcrops appear to contain the same sets as are found at depth, and thus provide insights into fracture patterns in deeply buried rocks. Spatial arrangement was investigated using variogram analysis. In the study area, the Utica Shale contains three sets of steeply dipping opening-mode fractures, bed-parallel fractures, and faults. Fracture sizes were also documented. Some fractures have heights of as much as 30 m. Length measurements were restricted by the small lateral extent of outcrops, but lengths of as much as 10 m were found. Outcrop analysis revealed strong tendencies for steeply dipping fractures to be bed-bounded, and partitioned by rock type, although some shale fractures are interpreted to be non-stratabound. Variogram analysis revealed evidence of clustering.

Lamarche et al. (2017b) studied the process of fracture interaction and hooking in Permian shales of the Lodève Basin (SW France). This process, related to fracture tip stress interaction, which ultimately connects fractures of similar orientations, can have a significant impact on the overall connectivity of a fracture network. The paper provides key geometric parameters at each of the three main stages of the hooking process—underlapping, overlapping and linkage—which mainly depend on the length and the spacing of the interacting fractures and the stress regime during fracture growth. They also suggest that such a process can occur at all fracture scales but that only fractures of similar sizes interact and link.

With a wide range of factors potentially influencing fracture formation and evolution in folds, resultant fracture networks can be complex and heterogeneous. Watkins et al. (2017) present a fracture dataset collected in outcrop for better constraining controls on fracture attributes and distributions in fold-thrust belts. Using the Achnashellach Culmination, Moine Thrust Belt, NW Scotland, the study documents the spatial distribution of fracture connectivity, orientation, and cement fill at different structural positions in several structures. A 3-D model, constructed using field observations and bedding data, and geomechanically restored using Move software, accounts for how factors such as fold curvature and strain influence fracture variation.

Fracture patterns are consistent and predictable in high strain forelimbs, marked by numerous, large, and interconnected fractures. However, in low-strain backlimbs connectivity is lower, and heterogeneities in connectivity and orientation do not correspond to fluctuations in strain or fold curvature. Here, other factors such as lithology have a greater control on fracture attribute distributions. Although fractures are less prevalent and less predictable in low strain regions, these fractures are predominantly open, whereas those in the high-strain areas are quartz filled. Thus, the concentration of the largest and most numerous fractures, in high strain zones, is markedly offset from the distribution of open fractures.

5.3. Faults and deformation bands

As noted above, Maerten et al. (2017) describe along-fault friction and fluid pressure effects on the spatial distribution of fault-related fractures. Using high-resolution 3D seismic data from a deep water setting near Malaysia, Totake et al. (2017) analyze structural variations along strike in a deep-water thrust belt with the aim of assessing along-strike patterns of fault heave and elevation of thrust hangingwalls. Kinematic interactions and linkages between fold-thrust structures cause along strike changes in fold and thrust geometry. Local heave deficits on large master thrusts are compensated by the occurrence of small imbricate thrust arrays and increased fold strain. Relays of displacement lead to complex but systematic cross-strike patterns. The patterns and mapping approach used provides a way to infer the presence of local complex multiple faults in less well-imaged parts of seismic volumes.

The spatial arrangement of faults is an area of continuing concern, where new and improved methods are being applied, for example as noted above with respect to the study by Hanke et al. (2017). The spatial arrangement and size patterns of faults in a supra-detachment basin was examined by Laubach et al. (2017) using the Marrett et al. (2017) normalized correlation count method as well as standard methods. Normalized correlation count reveals that in this high-strain fault pattern, instead of interaction among faults during their propagation boundary conditions such as fault shape, mechanical unit thickness and internal stratigraphy on a range of scales influence spatial and size patterns.

Considering deformation bands, most literature focuses on siliciclastic rocks, leaving a gap regarding carbonate-hosted deformation bands. Lubiniecki et al. (2017) focuses on the mechanisms involved in carbonate-hosted deformation bands and attempt to link their coevolution with fractures in the adjacent shale

formation in the St. Vincent Basin. They investigated the Oligocene-Miocene calcarenites of Port Willunga Formation, which is offset by the NE-SW striking curvilinear Willunga Fault at Sellicks Beach, South Australia. The Willunga Fault is a steep southeast dipping reverse fault at present-day, which reactivated from an original half-graben structure formed during the final separation of Antarctica from Australia in the middle Eocene. Mapping 221 carbonate-hosted deformation bands within the footwall and 440 shale-hosted fractures within the hanging wall of the Willunga Fault suggests that carbonate-hosted deformation bands have a range of cataclasis intensity, which is defined by the degree of comminution and bioclast alignment within the deformation band that results in 25–33% porosity reduction. Iron-hydroxide cement further reduces band porosity by 1%. Furthermore, their results indicate that deformation bands provide useful evidence for constraining the structural evolution of basins over neotectonic timescales.

A challenge to understanding fluid flow in buried basement rocks is that only the largest faults are generally visible to basin-scale geophysical investigations. Three papers address the spatial arrangement of faults and fractures in basement rocks over a range of scales and resolutions. Using the western shoulder of the Upper Rhine Graben as an example, Bertrand et al. (2017) show how structural heritage and rock type variations govern spatial arrangement of reactivation and distribution of fault and fracture networks in a rift setting. Scanlines, outcrop mapping, digital terrain models and regional data show a hierarchy of fault blocks that control the fine-scale structures. Controls on orientations, lengths, spacing and densities are a combination of neo-formed and reactivated older structures interacting with rock type.

Based on crystalline basement rocks of the southern Black Forest, Germany, Meixner et al. (2017) explore spatial patterns using digital elevation models and satellite imagery. Results have implications for identification and spatial arrangement of lineaments and fault zones in crystalline rocks. They map lineaments over an area of 2000 km^2 and compare results derived from different image types. The quantities assessed include orientation, average length, and total length of linear feature. Statistical analysis shows that differences in resolution distinctly impacts results. For each type of representation, the authors are able to define the censoring bias and truncation bias on observable lineament length. This study is an example of documentation of spatial patterns on a broad scale. The authors were able to correlate lineaments with faults. They found differences in fault density corresponding to host rock types, with higher fault density in granite-dominated areas and lower fault density where gneiss is prevalent. Geomechanical slip-tendency analysis applied to the fault pattern assesses which faults might be present and critically stressed in basement rocks.

Turning to the spatial arrangement of faults and fracture zones on a wide regional scale, Gabrielsen et al. (2017) describe fault distributions in the Precambrian basement of South Norway. Remote sensing methods and potential field data and local high-resolution field studies illuminate brittle basement structures on the scale of a large crustal block. A regular pattern visible on this broad scale encompasses faults and fracture zones of different age, style, attitude, and frequency.

5.4. Spatial variability, connectivity and fluid flow

The spatial distribution of structures is a major source of heterogeneity in rocks and, hence, in the uncertainty in predicting geological processes. In this volume, new approaches are presented for understanding and quantifying spatial distribution over a wide range of scales. Many contributions use well-constrained surface exposures, which provide insights and the opportunity to test new ideas. In the sub-surface, information is generally sparse due to the small volume sampled by wells and the limited seismic resolution of small features. Thus, predicting the spatial arrangement of fractures at the scale of an entire structure object from field analogues can provide valuable constraints when extrapolating beyond well control (Bruna et al., 2015). However, it is important to remember that surface exposures may have quite different deformation histories to similar rock in the sub-surface (Laubach et al., 2009; Sanderson, 2015). For example, many barren fractures (joints) develop during the late uplift or surface history of rocks and may be absent, or have different character due to solution and cementation in the sub-surface.

Differences in spatial arrangement have implications for reservoir characterization. Fracture clusters (or corridors) have been identified as widespread features in both groundwater and hydrocarbon reservoir rocks (e.g., Questiaux et al., 2010) that need to be accounted for in reservoir modeling. In Li et al.'s (2017) subsurface example, core observations show that two orthogonal fracture sets are open and capable of contributing to fluid flow. Analysis of long image-log data sets shows that clustering characterizes both sets. Interconnections between clusters of the same or different sets could impact flow patterns. Clusters separated by unfractured or less fractured rock could, for example, explain differences between gas and water production from nearby wells.

From a petroleum industry standpoint, a naturally fractured reservoir (NFR) is one in which open fractures may enhance the permeability field, thereby affecting well productivity and recovery efficiency (Narr et al., 2006). In such reservoirs, experience suggests that there is a disconnect between the 'fracture network' comprising all the fractures present in the reservoir at all scales, and the 'flow network' consisting only of open and, in some sense, connected fractures that affect the flow on timescales of well production. This issue is also pertinent to flow in fractures in geothermal reservoirs and in waste disposal and sequestration applications. There are many reasons for such discrepancies. One being the tendency for some fractures, or parts of fractures, to fill with cement (i.e., Laubach, 2003; Olson et al., 2009). As illustrated by the Hooker et al. (2017) study, the geochemical aspects of how fracture systems grow and how they alter with time are topics that are ripe for further investigation with new spatial analysis tools in combination with other approaches.

Outcrop imaging of fracture traces can usefully incorporate a component of fracture petrology to unravel the porosity history of the fracture arrays, rather than treating all the traces as open fractures. The arrangement as well as the geometry of exchange between the matrix and the fractures, and porosity characteristics of fractures over a range of scales governs how ultimately the different fracture scales should be represented in flow simulation models. Patterns and size distributions may have invariant geometric properties over a wide range of scales (e.g., Sanderson and Nixon, 2015) whereas porosity structures may vary abruptly owing to geochemical effects. For example, Marrett et al. (2017) show that aperture size distributions are well described by a single power law over four orders of magnitude, but that the fracture cement history shows that only the largest fractures were open for fluid flow, with all fractures later becoming sealed. Hooker et al. (2017) show that the spacing and spatial arrangement patterns themselves may depend on the geochemistry at the time of fracture growth as much as on mechanics considerations. Other recent studies support the importance of these interactions (Gillespie et al., 2001; Hooker et al., 2012, 2013).

Spatial arrangement, among other things, is a constraint on connectivity and therefore plays a vital role in the character of the flow network (Odling, 1997; Manzocchi, 2002; Ozkaya and Mattner, 2003). In subsurface rocks having finite, even if low, permeability,

fully interconnected fracture networks are not required to significantly affect flow on engineering timescales (Philip et al., 2005). But the character of near intersections such as in the hooking relations described by Lamarche et al. (2017a,b) can affect flow. Therefore, providing a static-dynamic calibration, the characterization of the spatial arrangement of fractures at all scales from limited, 1-D, well data is a key issue. For example, the definition of the characteristic dimensions of a clustered network or that of an homogenously distributed diffuse network (Roy et al., 2014; Marrett et al., 2017) combined with an understanding of the frequency and spatial distribution of fracture apertures from thin section data (Iñigo et al., 2012; Hooker et al., 2013) will allow better reconciliation of the characteristic dynamic parameters obtained from well tests and appropriate adjustments to the theoretical reservoir engineering flow laws (Denetto and Kamp, 2016).

6. Conclusions

Papers in this volume provide new results and a critical review of many aspects of previous work on spatial arrangement. Examples include studies of fault and fracture spatial arrangements in a wide range of rock types and structural settings, over a wide range of scales. Several studies point toward useful directions for further work. New approaches to documenting fault and fracture patterns include analytical approaches to quantify spatial arrangement, and rigorously identify clustering more concentrated than random. Illustrations of topological methods to document the full complexity of fracture arrays continue to show promise. Petrologic approaches that allow the time-sequence of development of fracture patterns adds a powerful new dimension to understanding how fracture patterns develop.

From the variety of papers in this volume it is clear that our understanding of the spatial arrangement of fractures is advancing rapidly. The path from fracture characterization to predicting fluid flow and other effects clearly involves three key considerations:

1) The measurement of geometrical attributes linked to the spatial location of the data and, hence, to the spatial variability of such attributes over a wide range of scales;
2) An understanding of how the individual fractures relate to one another (intersection, connectivity, etc.) in terms of the topology of the network (as in Fig. 7);
3) How the form and microstructure (aperture, cement, etc.) varies spatially and temporally and influences the transmissivity of the individual fractures or fracture sets (Fig. 7d).

Only by combining information from all three of these aspects is it possible to predict reliably the fluid flow, rock strength, and other key properties affected by fractures. Papers in this volume show that we should address these three elements together because spatial location, size, patterns, and the evolving geochemistry of host rock and fractures likely represent interacting systems.

Acknowledgments

SEL's work supported by grant DE-FG02-03ER15430 from Chemical Sciences, Geosciences and Biosciences Division, Office of Basic Energy Sciences, Office of Science, U.S. Department of Energy, and by the Fracture Research and Application Consortium. We are grateful to Qiqi Wang and Mark Shuster for comments on an early version of this paper.

References

Alzayer, Y., Eichhubl, P., Laubach, S.E., 2015. Non-linear growth kinematics of opening-mode fractures. J. Struct. Geol. 74, 31–44. http://dx.doi.org/10.1016/j.jsg.2015.02.003.
Anders, M.H., Laubach, S.E., Scholz, C.H., 2014. Microfractures: a review. J. Struct. Geol. 69B, 377–394. http://dx.doi.org/10.1016/j.jsg.2014.05.011.
Anderson, C.A., Hansen, A., Le Goc, R., Davy, P., Hope, S.M., 2013. Topology of fracture networks. Front. Phys. 1 http://dx.doi.org/10.3389/fphy.2013.00007.
Ankit, K., Urai, J.L., Nestler, B., 2015. Microstructural evolution in bitaxial crack-seal veins: a phase-field study. J. Geophys. Res. Solid Earth 120 (5), 3096–3118.
Atkinson, B.K., 1984. Subcritical crack growth in geological materials. J. Geophys. Res. 89, 4077–4114.
Aydin, A., 2000. Fractures, faults, and hydrocarbon entrapment, migration and flow. Mar. Pet. Geol. 17, 797–814.
Bai, T., Pollard, D.D., 2000. Fracture spacing in layered rocks: a new explanation based on the stress transition. J. Struct. Geol. 22 (1), 43–57.
Bai, T., Pollard, D.D., Gao, H., 2000. Explanation for fracture spacing in layered materials. Nature 403, 753–756. http://dx.doi.org/10.1038/35001550.
Bear, J., Tsang, C.F., De Marsily, G., 2012. Flow and Contaminant Transport in Fractured Rock. Academic Press.
Belgrano, T.M., Herwegh, M., Berger, A., 2016. Inherited structural controls on fault geometry, architecture and hydrothermal activity: an example from Grimsel Pass, Switzerland. Swiss J. Geosci. 109 (3), 345–364.
Bemis, S., Micklethwaite, S., Turner, D., James, M.R., Akciz, S., Thiele, S., Bangash, H.A., 2014. Ground-based and UAV-based photogrammetry: a multi-scale, high-resolution mapping tool for structural geology and paleoseismology. J. Struct. Geol. 69, 163–178. http://dx.doi.org/10.1016/j.jsg.2014.10.007.
Bertrand, L., Jusseaume, J., Géraud, Y., Diraison, M., Damy, P.-C., Navelot, V., Haffen, S., 2017. Structural heritage, reactivation and distribution of fault and fracture network in rifting context: case study of the western shoulder of the Upper Rhine Graben. J. Struct. Geol. SG-D-16–00259R1.
Bisdom, K., Nick, H.M., Bertotti, G., 2017. An integrated workflow for stress and flow modelling using outcrop-derived discrete fracture networks. Comput. Geosci. 103, 21–35.
Bonnet, E., Bour, O., Odling, N.E., Davy, P., Main, I., Cowie, P., Berkowitz, B., 2001. Scaling of fracture systems in geological media. Rev. Geophys. 29, 347–383.
Bour, O., Davy, P., 1999. Clustering and size distributions of fault patterns: theory and measurements. Geophys. Res. Lett. 26 (13), 2001–2004.
Brodie, K., Fettes, D., Harte, B., Schmid, R., 2007. Structural Terms Including Fault Rock Terms. Recommendations by the IUGS Subcommission, web version 01.02.07.
Brookins, D.G., 2012. Geochemical Aspects of Radioactive Waste Disposal. Springer Science & Business Media, Springer-Verlag, New York, 347 pp.
Bruna, P.-O., Guglielmi, Y., Viseur, S., Lamarche, J., Bildstein, O., 2015. Coupling fracture facies with in-situ permeability measurements to generate stochastic simulations of tight carbonate aquifer properties: example from the Lower Cretaceous aquifer, Northern Provence, SE France. J. Hydrol. 529, 737–753.
Cacas, M.C., Daniel, J.M., Letouzey, J., 2001. Nested geological modelling of naturally fractured reservoirs. Pet. Geosci. 7, 43–52.
Caputo, R., Hancock, P.L., 1998. Crack-jump mechanism of microvein formation and its implications for stress cyclicity during extension fracturing. J. Geodyn. 27 (1), 45–60.
Chester, F.M., Logan, J.M., 1986. Implications for mechanical-properties of brittle faults from observations of the Punchbowl fault zone, California. Pure Appl. Geophys. 124, 79–106.
Cho, Y., Ozkan, E., Apaydin, O.G., 2013. Pressure-dependent natural-fracture permeability in shale and its effect on shale-gas well production. SPE Reserv. Eval. Eng. 16 (02), 216–228.
Choi, J.H., Edwards, P., Ko, K., Kim, Y.S., 2016. Definition and classification of fault damage zones: a review and a new methodological approach. Earth Sci. Rev. 152, 70–87.
Corradetti, A., Tavani, S., Parente, M., Iannace, A., Vinci, F., Pirmez, C., Torrieri, S., Giorgioni, M., Pignalosa, A., Mazzoli, S., 2017. Distribution and arrest of vertical through-going joints in a reservoir-scale carbonate platform exposure (Sorrento peninsula, Italy): insights from integrating field survey and digital outcrop model. J. Struct. Geol. SG-D-16–00268R1.
Couples, G.D., Lewis, H., 1998. Lateral variations of strain in experimental forced folds. Tectonophysics 295, 79–91.
Cowie, P.A., Scholz, C.H., 1992. Growth of faults by accumulation of seismic slip. J. Geophys. Res. 97, 11085–11095.
Dahi-Taleghani, A., Olson, J.E., 2011. Numerical modeling of multistranded-hydraulic-fracture propagation: accounting for the interaction between induced and natural fractures. SPE J. 16 (03), 575–581.
Delaney, P.T., Pollard, D.D., Ziony, J.I., McKee, E.H., 1986. Field relations between dikes and joints: emplacement processes and paleostress analysis. J. Geophys. Res. Solid Earth 91 (B5), 4920–4938.
Denetto, S., Kamp, A.M., 2016. Cubic Law Evaluation Using Well Test Analysis for Fractures Reservoir Characterization. SPE-181410-MS.
Dershowitz, W., Hermanson, J., Follin, S., Mauldon, M., 2000. Fracture intensity measures in 1-D, 2-D, and 3-D at Äspö, Sweden. In: Girard, J.M., Liebman, I., Breeds, A., Doe, T. (Eds.), 4th North American Rock Mechanics Symposium. American Rock Mechanics Association, Balkema, Rotterdam, pp. 849–853.
Engelder, T., 1985. Loading paths to joint propagation during a tectonic cycle: an example from the Appalachian Plateau, USA. J. Struct. Geol. 7 (3), 459–476.
English, J.M., Laubach, S.E., 2017. Opening-mode fracture systems – insights from recent fluid inclusion microthermometry studies of crack-seal fracture cements. In: Turner, J.P., Healy, D., Hillis, R.R., Welch, M. (Eds.), Geomechanics and

Geology. Geological Society, London, Special Publications, p. 458. http://dx.doi.org/10.1144/SP458.1.
Evans, M.A., 1995. Fluid inclusions in veins from the Middle Devonian shales: a record of deformation conditions and fluid evolution in the Appalachian Plateau. Geol. Soc. Am. Bull. 107 (3), 327–339.
Evans, M.A., Fischer, M.P., 2012. On the distribution of fluids in folds: a review of controlling factors and processes. J. Struct. Geol. 44, 2–24. http://dx.doi.org/10.1016/j.jsg.2012.08.003.
Gabrielsen, R.H., Nystuen, J.P., Olesen, O., 2017. Fault distribution in the precambrian basement of South Norway. J. Struct. Geol. http://dx.doi.org/10.1016/j.jsg.2017.06.006.
Gabrielsen, R.H., Braathen, A., 2014. Models of fracture lineaments—Joint swarms, fracture corridors and faults in crystalline rocks, and their genetic relations. Tectonophysics 628, 26–44.
Gale, J.F.W., Laubach, S.E., Olson, J.E., Eichhubl, P., Fall, A., 2014. Natural fractures in shale: a review and new observations. AAPG Bull. 98 (11), 2165–2216. http://dx.doi.org/10.1306/08121413151.
Gillespie, P., Casini, G., Iben, H., O'Brien, J.F., 2017. Simulation of subseismic joint and fault networks using a heuristic mechanical model. In: Ashton, M., Dee, S.J., Wennberrg, O.P. (Eds.), Subseismic-scale Reservoir Deformation, vol. 459. Geological Society, London. http://dx.doi.org/10.1144/SP459.6. Special Publication.
Gillespie, P.A., Howard, C.B., Walsh, J.J., Watterson, J., 1993. Measurement and characterization of spatial distributions of fractures. Tectonophysics 226, 114–141.
Gillespie, P.A., Johnston, J.D., Loriga, M.A., McCaffrey, K.J.W., Walsh, J.J., Watterson, J., 1999. Influence of layering on vein systematics in line samples. In: McCaffrey, K.J.W., Lonergan, L., Wilkinson, J.J. (Eds.), Fractures, Fluid Flow and Mineralisation, 155. Geological Society, London, Special Publication, pp. 35–56.
Gillespie, P.A., Walsh, J.J., Watterson, J., Bonson, C.G., Manzocchi, T., 2001. Scaling relationships of joint and vein arrays from the Burren, Co. Clare, Ireland. J. Struct. Geol. 23, 183–201.
Gomez, L.A., Laubach, S.E., 2006. Rapid digital quantification of microfracture populations. J. Struct. Geol. 28 (3), 408–420. http://dx.doi.org/10.1016/j.jsg.2005.12.006.
Gross, M.R., 1993. The origin and spacing of cross joints: examples from Monterey Formation, Santa Barbara Coastline, California. J. Struct. Geol. 15, 737–751.
Guerriero, V., Vitale, S., Ciarcia, S., Mazzoli, S., 2011. Improved statistical multi-scale analysis of fractured reservoir analogues. Tectonophysics 504 (1–4), 14–24. http://dx.doi.org/10.1016/j.tecto.2011.01.003.
Hanke, J.R., Fischer, M.P., Pollyea, R.M., 2017. Directional semivariogram analysis to identify and rank controls on the spatial variability of fracture networks. J. Struct. Geol. SG-D-17–00018.
Hardebol, N.J., Bertotti, G., 2013. DigiFract: a software and data model implementation for flexible acquisition and processing of fracture data from outcrop. Comput. Geosci. 54, 326–336.
Healy, D., Rizzo, R.E., Cornwell, D.G., Farrell, N.J., Watkins, H., Timms, N.E., Gomez-Rivas, E., Smith, M., 2017. FracPaQ: a MATLAB™ toolbox for the quantification of fracture patterns. J. Struct. Geol. 95, 1–16.
Hilgers, C., Kirschner, D.L., Breton, J.P., Urai, J.L., 2006. Fracture sealing and fluid overpressures in limestones of the Jabal Akhdar dome, Oman Mountains. Geofluids 6 (2), 168–184.
Holland, M., Urai, J.L., 2010. Evolution of anastomosing crack–seal vein networks in limestones: insight from an exhumed high-pressure cell, Jabal Shams, Oman Mountains. J. Struct. Geol. 32 (9), 1279–1290.
Hooker, J.N., Katz, R.F., 2015. Vein spacing in extending, layered rock: the effect of synkinematic cementation. Am. J. Sci. 315, 557–588.
Hooker, J.N., Gale, J.F.W., Gomez, L.A., Laubach, S.E., Marrett, R., Reed, R.M., 2009. Aperture-size scaling variations in a low-strain opening-mode fracture set, Cozzette Sandstone, Colorado. J. Struct. Geol. 31 (7), 707–718. http://dx.doi.org/10.1016/j.jsg.2009.04.001.
Hooker, J.N., Gomez, L.A., Laubach, S.E., Gale, J.F.W., Marrett, R., 2012. Effects of diagenesis (cement precipitation) during fracture opening on fracture aperture-size scaling in carbonate rocks. In: Garland, J., Neilson, J.E., Laubach, S.E., Whidden, K.J. (Eds.), Advances in Carbonate Exploration and Reservoir Analysis, vol. 370. Geological Society, London, pp. 187–206. Special Publication.
Hooker, J.N., Laubach, S.E., Marrett, R., 2017. Microfracture spacing distributions and the evolution of fracture patterns in sandstones. J. Struct. Geol. http://dx.doi.org/10.1016/j.jsg.2017.04.001.
Hooker, J.N., Laubach, S.E., Marrett, R., 2013. Fracture-aperture size–frequency, spatial distribution, and growth processes in strata-bounded and non-strata-bounded fractures, Cambrian Mesón Group, NW Argentina. J. Struct. Geol. 54, 54–71.
Huang, Q., Angelier, J., 1989. Fracture spacing and its relation to bed thickness. Geol. Mag. 126 (4), 355–362.
Iñigo, J.F., Laubach, S.E., Hooker, J.N., 2012. Fracture abundance and patterns in the Subandean fold and thrust belt, Devonian Huamampampa Formation petroleum reservoirs and outcrops, Argentina and Bolivia. Mar. Pet. Geol. 35 (1), 201–218. http://dx.doi.org/10.1016/j.marpetgeo.2012.01.010.
Ivanova, V.M., Sousa, R., Murrihy, B., Einstein, H.H., 2014. Mathematical algorithm development and parametric studies with the GEOFRAC three-dimensional stochastic model of natural rock fracture systems. Comput. Geosci. 67, 100–109.
Jelsma, H.A., De Wit, M.J., Thiart, C., Dirks, P.H., Viola, G., Basson, I.J., Anckar, E., 2004. Preferential distribution along transcontinental corridors of kimberlites and related rocks of Southern Africa. South Afr. J. Geol. 107 (1–2), 301–324.
Jourde, H., Flodin, E.A., Aydin, A., Durlofsky, L.J., Wen, X.-H., 2002. Computing permeability of fault zones in eolian sandstone from outcrop measurements. AAPG Bull. 86, 1187–1200.
Kim, Y.S., Peacock, D.C.P., Sanderson, D.J., 2004. Fault damage zones. J. Struct. Geol. 26, 503–517.
Korneva, I., Bastesen, E., Corlett, H., Eker, A., Hirani, J., Hollis, C., Gawthorpe, R.L., Rotevatn, A., Taylor, R., 2017. The effects of dolomitization on petrophysical properties and fracture distribution within rift-related carbonates (Hammam Faraun Fault Block, Suez Rift, Egypt). J. Struct. Geol. http://dx.doi.org/10.1016/j.jsg.2017.06.005.
Kruhl, J.H., 2013. Fractal-geometry techniques in the quantification of complex rock structures: a special view on scaling regimes, inhomogeneity and anisotropy. J. Struct. Geol. 46, 2–21. http://dx.doi.org/10.1016/j.jsg.2012.10.002.
Kuiper, N.H., 1960. Tests concerning random points on a circle. In: Proceedings of the Koninklijke Nederlandse Akademie van Wetenschappen (A), vol. 63, pp. 38–47.
La Pointe, P.R., Hudson, J.A., 1985. Characterization and Interpretation of Rock Mass Joint Patterns, vol. 199. Geological Society of America, Denver, Colorado. Special Paper.
Ladeira, F.L., Price, N.J., 1981. Relationship between fracture spacing and bed thickness. J. Struct. Geol. 3, 179–183.
Ladevèze, P., Séjourné, S., Rivard, C., Lavoie, D., Lefebre, R., Rouleau, A., 2017. Defining the natural fracture network in a shale gas play and its cover succession: the case of the Utica Shale in eastern Canada. J. Struct. Geol. SG-D-17–00079.
Lamarche, J., Chabani, A., Gauthier, B.D.M., 2017a. Process of fracture linkage and hooking. J. Struct. Geol. SG-D-17-00019.
Lamarche, J., Viseur, S., Chatalée, S., Bachtarzi, N., Fleury, J., 2017b. Characterization of fracture corridors from digital outcrop by combining automatic detection approaches with field analysis. In: Value of Virtual Outcrops in Geosciences; 79th EAGE Conference and Exhibition, Paris 12 June 2017.
Lander, R.H., Laubach, S.E., 2015. Insights into rates of fracture growth and sealing from a model for quartz cementation in fractured sandstones. Geol. Soc. Am. Bull. 127 (3-4), 516–538. http://dx.doi.org/10.1130/B31092.1.
Laubach, S.E., Mace, R.E., Nance, H.S., 1995. Fault and joint swarms in a normal fault zone. In: Rossmanith, H.-P. (Ed.), Mechanics of Jointed and Faulted Rock. Balkema, Rotterdam, pp. 305–309.
Laubach, S.E., Marrett, R., Olson, J., Scott, A.R., 1998. Characteristics and origins of coal cleat: a review. Int. J. Coal Geol. 35 (1–2), 175–207. http://dx.doi.org/10.1016/S0166-5162(97)00012-8.
Laubach, S.E., 1992. Fracture networks in selected cretaceous sandstones of the green river and San Juan basins, Wyoming, New Mexico, and Colorado. In: Schmoker, J.W., Coalson, E.B., Brown, C.A. (Eds.), Geological Studies Relevant to Horizontal Drilling: Examples from Western North America. The Rocky Mountain Association of Geologists, Denver, pp. 115–127.
Laubach, S.E., 2003. Practical approaches to identifying sealed and open fractures. AAPG Bull. 87, 561–579.
Laubach, S.E., Eichhubl, P., Hargrove, P., Ellis, M.A., Hooker, J.N., 2014. Fault core and damage zone fracture attributes vary along strike owing to interaction of fracture growth, quartz accumulation, and differing sandstone composition. J. Struct. Geol. 68A, 207–226. http://dx.doi.org/10.1016/j.jsg.2014.08.007.
Laubach, S.E., Fall, A., Copley, L.K., Marrett, R., Wilkins, S.J., 2016. Fracture porosity creation and persistence in a basement-involved laramide fold, upper cretaceous Frontier Formation, Green river basin, USA. Geol. Mag. 153, 887–910. http://dx.doi.org/10.1017/S0016756816000157.
Laubach, S.E., Hundley, T.H., Hooker, J.N., Marrett, R., 2017. Spatial arrangement and size distribution of normal faults, Buckskin Detachment upper plate, Western Arizona. J. Struct. Geol.
Laubach, S.E., Olson, J.E., Gross, M.R., 2009. Mechanical and fracture stratigraphy. AAPG Bull. 93 (11), 1413–1426. http://dx.doi.org/10.1306/07270909094.
Lavenu, A.P., Lamarche, J., 2017. What controls diffuse fractures in platform carbonates? Insights from Provence (France) and Apulia (Italy). J. Struct. Geol. http://dx.doi.org/10.1016/j.jsg.2017.05.011.
Li, J.Z., Laubach, S.E., Gale, J.F.W., Marrett, R.A., 2017. Quantifying opening-mode fracture spatial organization in horizontal wellbore image logs, core and outcrop: application to Upper Cretaceous Frontier Formation tight gas sandstones, USA. J. Struct. Geol. http://dx.doi.org/10.1016/j.jsg.2017.04.001.
Lorenz, J.C., Hill, R.E., 1994. Subsurface fracture spacing: comparison of inferences from slant/horizontal core and vertical core in Mesaverde reservoirs. SPE Form. Eval. 9 (01), 66–72.
Lubiniecki, D.C., White, S.R., King, R.C., Holford, S.P., Bunch, M.A., Hill, S., 2017. Structural evolution of carbonate-hosted deformation bands adjacent to a major neotectonic fault: Sellicks Beach, South Australia. J. Struct. Geol. SG-D-17–00025.
Maerten, L., Maerten, F., Lejri, M., 2017. Along fault friction and fluid pressure effects on the spatial distribution of fault-related fractures. J. Struct. Geol. SG-D-17–00068.
Manzocchi, T., 2002. The connectivity of two-dimensional networks of spatially correlated fractures. Water Resour. Res. 38 (9), 1162. http://dx.doi.org/10.1029/2000WR000180.
Marrett, R., Gale, J.F.W., Gomez, L.A., Laubach, S.E., 2017. Correlation analysis of fracture arrangement in space. J. Struct. Geol. http://dx.doi.org/10.1016/j.jsg.2017.06.012.
Matonti, C., Lamarche, J., Guglielmi, Y., Marie, L., 2012. Characterization of mixed conduit/seal fault zones in carbonates: example from the Castellas fault (SE

France). J. Struct. Geol. 39, 103–121.
Mauldon, M., Dunne, W.M., Rohrbaugh, M.B., 2001. Circular scanlines and circular windows: new tools for characterizing the geometry of fracture traces. J. Struct. Geol. 23 (2), 247–258.
McGinnis, R.N., Ferrill, D.A., Morris, A.P., Smart, K.J., Lehrmann, D., 2017. Mechanical stratigraphic controls on natural fracture spacing and penetration. J. Struct. Geol. 95, 160–170.
McGinnis, R.N., Ferrill, D.A., Smart, K.J., Morris, A.P., Higuera-Diaz, C., Prawika, D., 2015. Pitfalls of using entrenched fracture relationships: fractures in bedded carbonates of the hidden valley fault zone, Canyon lake Gorge, Comal county, Texas. AAPG Bull. 99, 2221–2245.
Meixner, J., Grimmer, J.C., Becker, A., Schill, E., Kohl, T., 2017. Comparison of different digital elevation models and satellite imagery for lineament analysis: implications for identification and spatial arrangement of fault zones in crystalline basement rocks of the southern Black Forest. J. Struct. Geol. SG-D-16–00270.
Myers, R.D., Crawford, B.R., Barron, J.W., Huang, H., 2017. Predicting stress sensitive productivity of naturally fractured reservoirs in low strain environments. In: SPE Middle East Oil & Gas Show and Conference. Society of Petroleum Engineers. http://dx.doi.org/10.2118/183926-MS.
Narr, W., 1996. Estimating average fracture spacing in subsurface rock. AAPG Bull. 80, 1565–1586.
Narr, W., Lerche, I., 1984. A method for estimating subsurface fracture density in core. AAPG Bull. 68 (5), 637–648.
Narr, W., Suppe, J., 1991. Joint spacing in sedimentary rocks. J. Struct. Geol. 13, 1037–1048.
Narr, W., Schechter, D.S., Thompson, L.B., 2006. Naturally Fractured Reservoir Characterization. Society of Petroleum Engineers, Richardson, Texas, 112 pp.
Odling, N.E., 1992. Network properties of a two-dimensional natural fracture pattern. Pure Appl. Geophys. 138 (1), 95–114.
Odling, N.E., 1997. Scaling and connectivity of joint systems in sandstones from western Norway. J. Struct. Geol. 19 (10), 1257–1271.
Ogata, K., Senger, K., Braathen, A., Tveranger, J., 2014. Fracture corridors as seal-bypass systems in siliciclastic reservoir-cap rock successions: field-based insights from the Jurassic Entrada Formation (SE Utah, USA). J. Struct. Geol. 66, 162–187.
Olson, J.E., Laubach, S.E., Eichhubl, P., 2010. Estimating natural fracture producibility in tight gas sandstones: coupling diagenesis with geomechanical modeling. Lead. Edge 29 (12), 1494–1499.
Olson, J.E., Laubach, S.E., Lander, R.H., 2009. Natural fracture characterization in tight gas sandstones: integrating mechanics and diagenesis. AAPG Bull. 93 (11), 1535–1549.
Olson, J.E., 1993. Joint pattern development: effects of subcritical crack growth and mechanical interaction. J. Geophys. Res. 98 (B7), 12251–12265.
Olson, J.E., 2004. Predicting fracture swarms — the influence of subcritical crack growth and the crack-tip process zone on joint spacing in rock. In: Cosgrove, J.W., Engelder, T. (Eds.), The Initiation, Propagation, and Arrest of Joints and Other Fractures, vol. 231. Geological Society, London, pp. 73–87. Special Publication.
Ortega, O., Marrett, R., Laubach, S.E., 2006. A scale-independent approach to fracture intensity and average spacing measurement. AAPG Bull. 90, 193–208.
Ozkaya, S.I., Mattner, J., 2003. Fracture connectivity from fracture intersections in borehole image logs. Comput. Geosci. 29 (2), 143–153.
Peacock, D.C.P., 2004. Differences between veins and joints using the example of the Jurassic limestones of Somerset. In: Cosgrove, J.W., Engelder, T. (Eds.), The Initiation, Propagation, and Arrest of Joints and Other Fractures, vol. 231. Geological Society, London, pp. 209–221. Special Publication.
Peacock, D.C.P., Nixon, C.W., Rotevatn, A., Sanderson, D.J., Zuluaga, L.F., 2016. Glossary of fault and other fracture networks. J. Struct. Geol. 92, 12–29.
Philip, Z.G., Jennings Jr., J.W., Olson, J.E., Laubach, S.E., Holder, J., 2005. Modeling coupled fracture-matrix fluid flow in geomechanically simulated fracture networks. SPE Reserv. Eval. Eng. 8 (4), 300–309.
Pickering, G., Bull, J.M., Sanderson, D.J., 1995. Sampl. Power Law Distrib. Tectonophys. 248 (1–2), 1–20. http://dx.doi.org/10.1016/0040-1951(95)00030-Q.
Priest, S.D., 1993. Discontinuity Analysis for Rock Engineering. Chapman & Hall, New York.
Priest, S.D., Hudson, J.A., 1976. Discontinuity spacings in rock. Int. J. Rock Mech. 13, 135–148.
Procter, A., Sanderson, D.J., 2017. Spatial and layer-controlled variability in fracture networks. J. Struct. Geol. http://dx.doi.org/10.1016/j.jsg.2017.07.008.
Putz-Perrier, M.W., Sanderson, D.J., 2008a. Spatial distribution of brittle strain in layered sequences. J. Struct. Geol. 30 (1), 50–64.
Putz-Perrier, M.W., Sanderson, D.J., 2008b. The distribution of faults and fractures and their importance in accommodating extensional strain in Kimmeridge Bay, Dorset, United Kingdom. In: Wibberley, C.A.J., Kurz, W., Imber, J., Holdsworth, R.E., Collettini (Eds.), The Internal Structure of Fault Zones: Implications for Mechanical and Fluid-flow Properties, vol. 299. Geological Society of London, Special Publication, pp. 97–111.
Putz-Perrier, M.W., Sanderson, D.J., 2010. Distribution of faults and extensional strain in fractured carbonates of the North Malta Graben. AAPG Bull. 94 (4), 435–456. http://dx.doi.org/10.1306/08260909063.
Questiaux, J.M., Couples, G.D., Ruby, N., 2010. Fractured reservoirs with fracture corridors. Geophys. Prospect. 58, 279–295.
Rawnsley, K.D., Rives, T., Petti, J.P., Hencher, S.R., Lumsden, A.C., 1992. Joint development in perturbed stress fields near faults. J. Struct. Geol. 14 (8–9), 939–951.
Renshaw, C.E., Pollard, D.D., 1994. Numerical simulation of fracture set formation: a fracture mechanics model consistent with experimental observations. J. Geophys. Res. Solid Earth 99 (B5), 9359–9372.
Rives, T., Razack, M., Petit, J.-P., Rawnsley, K.D., 1992. Joint spacing: analogue and numerical simulations. J. Struct. Geol. 14, 925–937.
Rizzo, R.E., Healy, D., De Siena, L., 2017. Benefits of maximum likelihood estimators for fracture attribute analysis: implications for permeability and up-scaling. J. Struct. Geol. 95, 17–31.
Roy, A., Aydin, A., Mukerji, T., 2016. The influence of resolution on scale-dependent clustering in fracture spacing data. Interpretation 4 (3), T387–T394. http://dx.doi.org/10.1190/INT-2015-0179.1.
Roy, A., Perfect, E., Dunne, W.M., McKay, L.D., 2014. A technique for revealing scale-dependent patterns in fracture spacing data. J. Geophys. Res. Solid Earth 119 (7), 5979–5986.
Roy, A., Perfect, E., Dunne, W.M., Odling, N., Kim, J.W., 2010. Lacunarity analysis of fracture networks: evidence for scale-dependent clustering. J. Struct. Geol. 32 (10), 1444–1449.
Rutqvist, J., Rinaldi, A.P., Cappa, F., Jeanne, P., Mazzoldi, A., Urpi, L., Guglielmi, Y., Vilarrasa, V., 2016. Fault activation and induced seismicity in geological carbon storage–Lessons learned from recent modeling studies. J. Rock Mech. Geotech. Eng. 8 (6), 789–804.
Sahimi, M., 2011. Flow and Transport in Porous Media and Fractured Rock: from Classical Methods to Modern Approaches. John Wiley & Sons.
Sanderson, D.J., 2015. Field-based structural studies as analogues to sub-surface reservoirs. In: Bowman, M., Smyth, H.R., Good, T.R., Passey, S.R., Hirst, J.P.P., Jordan, C.J. (Eds.), The Value of Outcrop Studies in Reducing Subsurface Uncertainty and Risk in Hydrocarbon Exploration and Production, vol. 436. Geological Society London, Special Publications, pp. 207–217.
Sanderson, D.J., Nixon, C.W., 2015. The use of topology in fracture network characterization. J. Struct. Geol. 72, 55–66. http://dx.doi.org/10.1016/j.jsg.2015.01.005.
Sanderson, D.J., Roberts, S., Gumiel, P., 1994. A fractal relationship between vein thickness and gold grade in drill core from La Codosera, Spain. Econ. Geol. 89, 168–173.
Santos, R., Miranda, T., Barbosa, A., Gomes, I., Matos, G., Gale, J.F.W., Neumann, V., Guimarães, L., 2015. Characterization of natural fracture systems: analysis of uncertainty effects in linear scanline results. AAPG Bull. 99 (12), 2203–2219. http://dx.doi.org/10.1306/05211514104.
Schöpfer, M.P.J., Childs, C., Walsh, J.J., Manzocchi, T., 2016. Evolution of the internal structure of fault zones in three-dimensional numerical models of normal faults. Tectonophysics 666, 158–163.
Singh, S.K., Abu-Habbiel, H., Khan, B., Akbar, M., Etchecopar, A., Montaron, B., 2008. Mapping fracture corridors in naturally fractured reservoirs: an example from Middle East carbonates. First Break 26 (5), 109–113.
Snyder, M., Waldron, J.W.F., 2017. Fracture overprinting history using Markov chain analysis: Windsor-Kennetcook subbasin, Maritimes Basin, Canada. J. Struct. Geol. http://dx.doi.org/10.1016/j.jsg.2017.07.009.
Solano, N., Zambrano, L., Aguilera, R., 2011. Cumulative-gas-production distribution on the Nikanassin tight gas formation, Alberta and British Columbia, Canada. SPE Reserv. Eval. Eng. 14, 357–376. http://dx.doi.org/10.2118/132923-PA.
Stephens, M.A., 1965. The goodness-of-fit statistic VN: distribution and significance points. Biometrika 52 (3/4), 309–321.
Terzaghi, R., 1965. Sources of error in joint surveys. Geotechnique 15, 287–297.
Totake, Y., Butler, R.W.H., Bond, C.E., Aziz, A., 2017. Analyzing structural variations along strike in a deep-water thrust belt. J. Struct. Geol. http://dx.doi.org/10.1016/j.jsg.2017.06.007.
Vandeginste, V., John, C.M., Beckert, J., 2015. Diagenetic geobodies: fracture-controlled burial dolomite in outcrops from northern Oman. SPE Reserv. Eval. Eng. 18 (01), 84–93.
Vidal, J., Genter, A., Chopin, F., 2017. Permeable fracture zones in the hard rocks of the geothermal reservoir at Rittershoffen, France. J. Geophys. Res. Solid Earth. http://dx.doi.org/10.1002/2017JB014331.
Vollgger, S.A., Cruden, A.R., 2016. Mapping folds and fractures in basement and cover rocks using UAV photogrammetry, Cape Liptrap and Cape Paterson, Victoria, Australia. J. Struct. Geol. 85, 168–187.
Walsh, J.J., Watterson, J., 1993. Fractal analysis of fracture patterns using the standard box-counting technique: valid and invalid methodologies. J. struct. Geol. 15 (12), 1509–1512.
Watkins, H., Bond, C.E., Healy, D., Butler, R.W., 2015. Appraisal of fracture sampling methods and a new workflow to characterise heterogeneous fracture networks at outcrop. J. Struct. Geol. 72, 67–82.
Watkins, H., Healy, D., Bond, C.E., Butler, R.W.H., 2017. Implications of heterogeneous fracture distribution on reservoir quality; an analogue from the Torridon Group sandstone, Moine Thrust Belt, NW Scotland. J. Struct. Geol. http://dx.doi.org/10.1016/j.jsg.2017.06.002.
Wehunt, D., Borovykh, M., Narr, W., 2017. Stochastic 2D well-path assessments for naturally fractured carbonate reservoirs. SPE Reserv. Eval. Eng. http://dx.doi.org/10.2118/180468-PA.
Weng, X., Kresse, O., Cohen, C.E., Wu, R., Gu, H., 2011. Modeling of hydraulic-fracture-network propagation in a naturally fractured formation. SPE Prod. Oper. 26 (04), 368–9380.
Yılmaz, O., Derlet, P.M., Molinari, J.F., 2017. Damage cluster distributions in numerical concrete at the mesoscale. Phys. Rev. E 95 (4), 043002. http://dx.doi.org/10.1103/PhysRevE.95.043002.
Zeeb, C., Gomez-Rivas, E., Bons, P.D., Blum, P., 2013. Evaluation of sampling methods for fracture network characterization using outcrops. AAPG Bull. 97 (9), 1545–1566 (2013).